2016

Indirect-direct band transformation of few-layer BiOCl under biaxial strain

Zhongfei Xu
Beihang University

Weichang Hao
Beijing University, whao@buaa.edu.cn

Qianfan Zhang
Beihang University

Zhongheng Fu
Beihang University

Haifeng Feng
University of Wollongong, hf533@uowmail.edu.au

See next page for additional authors

Publication Details

Xu, Z., Hao, W., Zhang, Q., Fu, Z., Feng, H., Du, Y. & Dou, S. (2016). Indirect-direct band transformation of few-layer BiOCl under biaxial strain. The Journal of Physical Chemistry C: Energy Conversion and Storage, Optical and Electronic Devices, Interfaces, Nanomaterials, and Hard Matter, 120 (16), 8589-8594.

Indirect-direct band transformation of few-layer BiOCl under biaxial strain

Abstract
Being a new two-dimensional layered compounds, the tunable indirect-direct band transformation of BiOCl with different layers can be realized by introducing the biaxial tensile or compressive strains. The band structure and stability of BiOCl with different layers are first researched to clarify the influence of layer numbers. A phase transformation of bilayer BiOCl and metallic characteristic for all are observed under large tensile and compressive strains, respectively. In addition, bond length, interlayer spacing, and band decomposed charge density are calculated to analyze the mechanism behind these phenomena. The results indicate that the band structure transformation is primarily related to the competitions between two kinds of intralayer and interlayer Bi-O bonds and hybridizations between atoms under strains.

Keywords
layer, biocl, under, few, transformation, biaxial, band, strain, direct, indirect

Disciplines
Engineering | Physical Sciences and Mathematics

Publication Details
Xu, Z., Hao, W., Zhang, Q., Fu, Z., Feng, H., Du, Y. & Dou, S. (2016). Indirect-direct band transformation of few-layer BiOCl under biaxial strain. The Journal of Physical Chemistry C: Energy Conversion and Storage, Optical and Electronic Devices, Interfaces, Nanomaterials, and Hard Matter, 120 (16), 8589-8594.

Authors
Zhongfei Xu, Weichang Hao, Qianfan Zhang, Zhongheng Fu, Haifeng Feng, Yi Du, and S X. Dou

Indirect-Direct Band Transformation of Few-Layer BiOCl under Biaxial Strain

Zhongfei Xu[1,4], Weichang Hao[1, 4*], Qianfan Zhang[2,*], Zhongheng Fu[2], Haifeng Feng[3,4], Yi Du[3, 4], Shixue Dou[3,4]

[1]Department of Physics and Key Laboratory of Micro-nano Measurement, Manipulation and Physics, Ministry of Education (MOE), Beihang University, Beijing 100191, P. R. China

[2]School of Materials Science and Engineering, Beihang University, Beijing 100191, P. R. China

[3]Institute for Superconducting and Electronic Materials, University of Wollongong, Wollongong NSW 2522, Australia

[4]BUAA-UOWJoint Research Centre, Beihang University, Beijing 100191, P. R. China

Abstract: Being a new two-dimensional layered compounds, the tunable indirect-direct band transformation of BiOCl with different layers can be realizedby introducing the biaxial tensile or compressive strains. The band structure and stability of BiOCl with different layers are first researched to clarify the influence of layer numbers. A phase transformation of bilayer BiOCl and metallic characteristic for all are observed under large tensile and compressive strains, respectively. In addition, bond length, interlayer spacing, and band decomposed charge density are calculated to analyze the mechanism behind these phenomena. The results indicate that theband structure transformation is primarily related to the competitions between two kinds of intralayer and interlayer Bi-O bonds and hybridizations between atoms under strains.

Keywords: Biaxial Strain, Layered Structure, Band Structure, BiOCl

1. Introduction

Twodimensional (2D) layered materials, which consist of the interlayer van der Waals (vdW) interactions and intralayer covalent bonding, have inspired rapidly growing research efforts owing to their extraordinary properties and promising applications comparing with bulkcounterparts.[1-7]Recently, BiOX (X=Cl/Br/I) have attracted considerable interests as a new kind of 2D layered material with high visible-light photocatalytic activities due to its unique layered structure arranged in a X^--$[Bi_2O_2]^{2+}$-X^- configurations with vdW interactions between X atoms,as well as high chemical stability.[8-11]And to date, the thinnest ultrathin BiOCl nanosheet was synthesized with a thickness of 2.7 nm, which consisted of about four [Cl−Bi−O−Bi−Cl] units, by the group of Xie, their results show that solar-driven photocatalytic activities of ultrathin BiOCl nanosheet are obviously enhanced.[12] It has also been demonstrated by first-principle methods that the monolayer BiOX (except BiOF)with better photocatalytic activitiesare stable and the applied strains can improvetheir H_2 production by tuning the position of CBM.[13] Although experimental and theoretical explorations about BiOX have been extensively done,most of the reports focused on the photocatalytic properties.[14-16] In-depth studies on other aspects are still lacking, such as electronic structure designs of BiOX with a few layers. As is known to us all, strain is an effective method to tune the band structure for material design and improving performance.[17-20] For example, applied tensile strain can significantly enhance the electron mobility along zigzag direction and the biaxial strain can tune the optical band gap of monolayer black phosphorus.[21] Monolayer and bilayer MoS_2 change from semiconducting to metallic both under biaxial compressive and tensile strains.[22] Therefore, it is possible to tune the band structure while strains are applied on BiOX.[23]

In this paper, we researched the stability, electronic structures and bonding nature of BiOCl with different layers under both biaxial compressive and tensile strains using first-principle method. This work may help us take a deep look inside the material design for BiOX (X= Cl/Br/I).

2. Computational Methods

All calculations are performed using Vienna ab-initio simulation package (VASP) code. Generalized gradient approximation (GGA) was applied to treat the exchange correlation energy with the Perdew–Burke–Ernzerhof (PBE) functional. The Projector-augmented wave (PAW) method was employed to describe electron–ion interactions. The k-points sampling of 9×9×6 is generated with original Γ meshes. The cutoff energy for the plane wave basis is 550 eV. Equilibrium geometries were obtained by minimum energy principle until the force is converged to 0.01eV/Å. The biaxial strain ε from −25% to +30% with a step of 5%is applied equally in a and b directions. The strain ε is defined as

$$\varepsilon = \frac{a'-a}{a}$$

Here a' and a are respectively present the lattice constant with and without strain.

3. Results and Discussion

3.1. Crystal Structure and Formation Energy of BiOCl with Different Layers

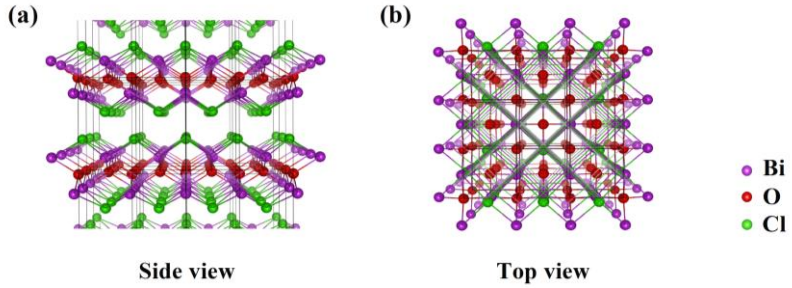

Figure1.Crystal structure of BiOCl: (a) side view; (b) top view.

BiOCl crystallizes as tetragonal structure with space group *P4/nmm* (space number 129), the crystal structure is showed in Figure 1.[24,25] In order to study the stability of BiOCl with different layers, theformation energies of bulk, 6-layer, 4-layer, 3-layer, bilayer, and monolayer are calculated. It can be expressed as[26,27]

$$E_f = \frac{E_{BiOCl} - n_{Bi}E_{Bi} - n_O E_O - n_{Cl}E_{Cl}}{N}$$

where E_f is the formation energy of crystals, E_{BiOCl} represent the total energy

of BiOCl. E_{Bi}, E_O, and E_{Cl} present the energies per atom of Bi, O, and Cl referenced to elemental solid/gas, respectively. n_{Bi}, n_O, and n_{Cl} are the number of Bi, O, Clatomsand N is the total number of atoms in crystals. The results are presented in Figure 2a, indicating that the stability of BiOCl decreases as a function of layer number which may be a possible reason why single-layer BiOCl is not obtained up to now where as the negative formation energies can ensure the favorable stability even for monolayer. As is to say, it is hopeful to synthesize single-layer BiOCl in future. The band gaps and band structures of bulk, 6-layer, 4-layer, 3-layer, bilayer, and monolayer BiOCl are calculated to clarify the influence of layer number on its electronic properties, as shown in Figure 2, parts a and b, respectively. Obviously, only a quantum size effect is observed and it is still an indirect-semiconductor for monolayer. In addition, the band structures exhibit an increasing band splitting while the layer number rises apart from that of bulk, this can be attribute to the reflection of both increasing size of the super cell and the presence of periodic vdW interactions in bulk but absence in multilayer along z axis.[28]

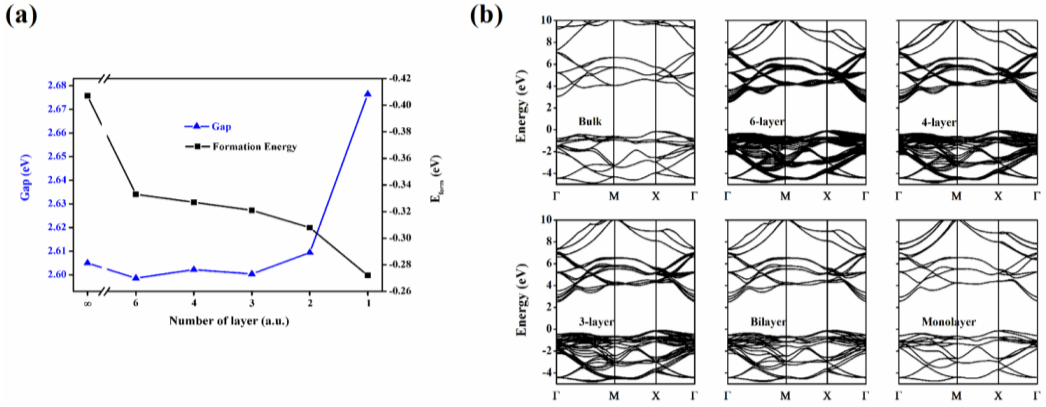

Figure 2. (a) Formation energy and band gap; (b) band structure of BiOCl with bulk, 6-layer, 4-layer, 3-layer, bilayer, and monolayer.

3.2. Band Structure of Layered BiOCl with Biaxial Tensile and Compressive Strains

On the Bases of the results discussed in section 3.1, bilayer can beregarded as an example for multilayer and bulk is taken for a comparison since the little differences are found among the band structures of bulk, multilayer and monolayer. Specifically, the crystal structures of bilayer under strain 0%, 25%, and 30% showed in Figure

3strongly indicate the phase transformation under 25% or 30% once the relative sliding between layers and even bond broken are discovered.[29-32] This demonstrated that the lack of periodic vdW interactions have greater effects for crystal and electronic structures of bilayer under strain comparing with that of monolayer and bulk. For other conditions, we did not find any phase transformations but lattice changes. In order to ensuring their stabilities of the crystals under strains, the formation energy of monolayer, bilayer and bulk are showed in Figure S1. The results show that they are all stable from -10% to +15%. For large tensile (25% and 30%) and compressive (-25% to -15%) strains, their formation energies are positive which may indicate an unstable structure. However, they may still exist as a metastable phase because of their relative small values under large strains.[33] Otherwise, the lower formation energy of bilayer under tensile strain 25% and 30% than monolayer and bulk may result from their phase transformation.

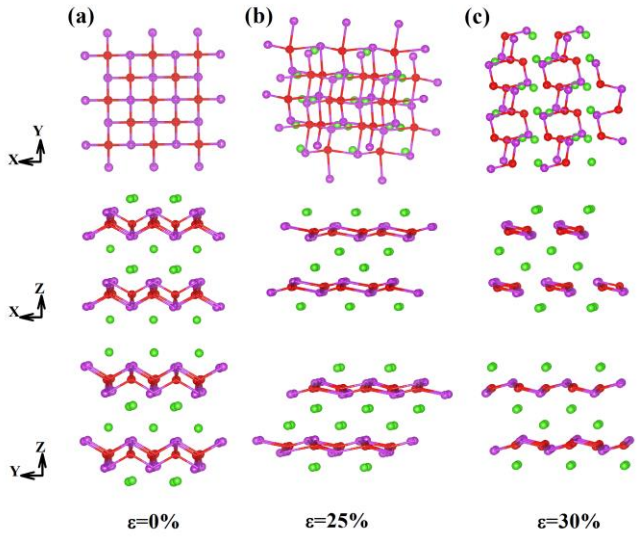

Figure3. Crystal structures of bilayer under tensile strain at (a) 0%, (b) 25%, and (c) 30%.

Some significant band structures of monolayer and bilayer under compressive, without and tensile strains -25%, -20%, -15%, 0%, +5%, +20%, +25%, +30% are presented in Figure 4. Apparently, the band structures transform between indirect and direct under both tensile and compressive strains. We can clearly see that the band structure of bilayer under strain 25% and 30% are quite different which induced by the phase transformation.

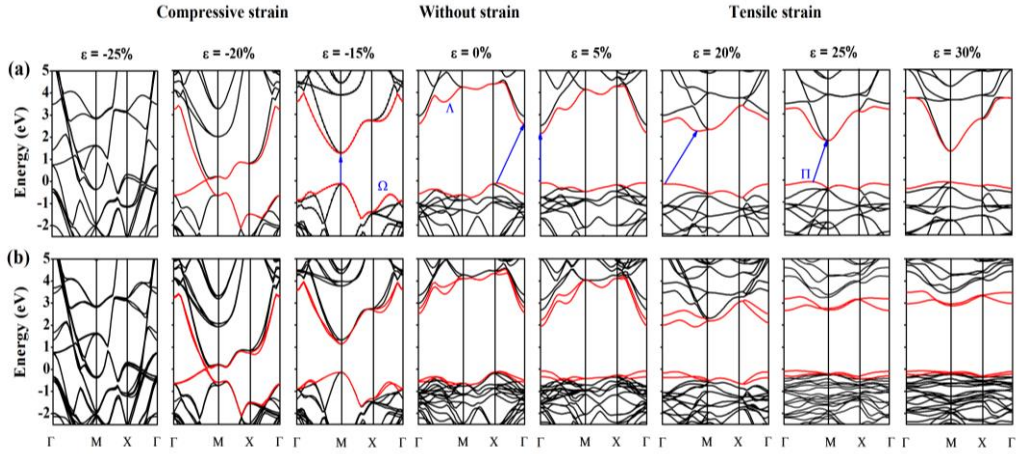

Figure 4. Band structure of (a) monolayer and (b) bilayer BiOCl under biaxial compressive, without and tensile strains.

3.2.1. Biaxial Tensile Strain

In the case of tensile strain, we can see that the band structure transform to direct band at Γwhile tensile strain is 5% for monolayer and bilayer, and become indirect band at 25% for monolayer but 20% for bilayer. In FigureS2, the band structure of bulk transform to direct band at 5% and indirect band at 10%. The differences of indirect-direct band transformation among crystals may result from the stronger sensibility of bulk with large tensile strains in contrast to monolayer and bilayer.

In Figure 3a, the indirect band to direct band transformations of monolayer are mainly caused by energy up-shifting or down-shifting at CBM-M, CBM-Λ (Λ is the point between Γ and M), VBM-Γ and VBM-Π (Π is the point between Γ and M) under tensile strains. Continuous falling of CBM-M and CBM-Λ finally lead to the change of CBM. Particularly, CBM-Λ becomes the lowest at 20%. These enable the conversion of CBM from Γ to Λ to M under tensile strain. Otherwise, the alternative variation between VBM-Γ and VBM-Π at 5% and 25% lead to VBM turns from Ω (the point between X and Γ) to Γ to Π. The similar phenomena are found in bilayer (Figure 3b) and bulk (Figure S2) except for different critical point of indirect-direct band transformation.

3.2.2. Biaxial Compressive Strain

For the band structure transformation of monolayer under compressive strains showed in Figure3a is mainly determined by the moving of CBM-M, VBM-Ω and VBM-M. It transforms to direct band at M as strain is increased to -15%, and displays a metallic character after -20%.Moreover, the continuous downshift of CBM-M make the CBM transforms from Γ to M under the compressive strains and the suddenly reducing of Ω at -15% induced VBM transformation from Ω to M.

Consequently, based on the analysis above all, changes of edge states on these k points result in the band structure transforms from indirect band to direct band, and finally change into metallic state under compressive strains. The similar tendencies are found in bilayer and bulkunder compressive strains (Figure S2).

3.3. Bonding Characters of Layered BiOCl with Biaxial Tensile and Compressive Strains

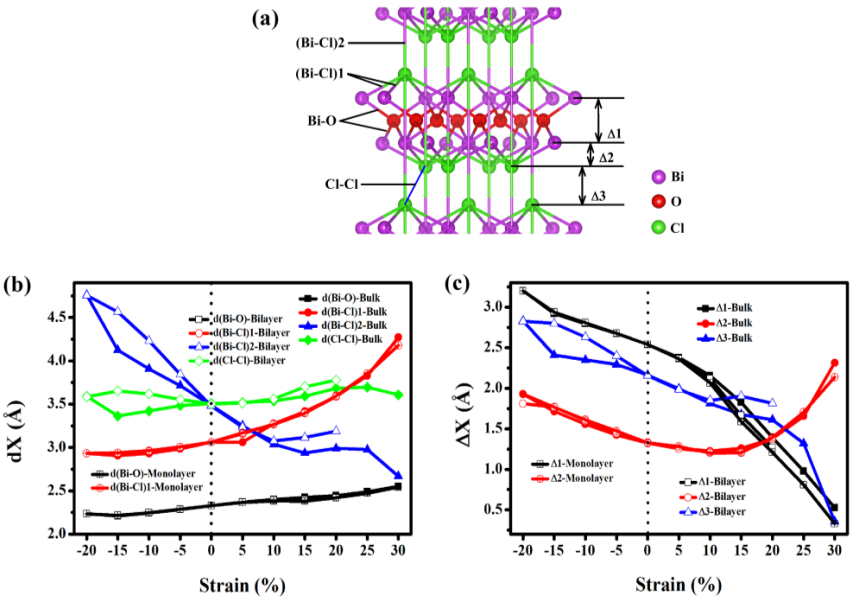

Figure5. (a) Schematic illustrations of bond length and interlamellar spacings, (b) bond length dX, (c) interlamellar spacings ΔX of bulk, bilayer, and monolayer under tensile and compressive strains. Purple, red, green atoms respectively refer to Bi, O, and Cl atoms.

Generally speaking, both bonding nature and layer distance are important factors which could affect the electronic structures in layered crystals.[34,35] The bond lengths,

angle and the interlayer spacing are calculated for analyzing the variation of band structure under strains, as shown in Figure5 and FigureS3. We calculated two kinds of intralayer bonds Bi-O and (Bi-Cl)1, two kinds of interlayer bonds (Bi-Cl)2 and Cl-Cl (It may not be exactly viewed as chemical bond because of the large Cl-Cl distance, but we define it as bond for simplicity). Figure5b shows that strain has a great influence on Bi-Cl bonds, (Bi-Cl)1 increases while (Bi-Cl)2 decreases from compressive strain to tensile strain. It is noticeable that (Bi-Cl)1 is longer than (Bi-Cl)2 after 10%, and it becomes the longest bond (which may have been broken) among all bonds after 20% and even larger than Cl-Cl. The results suggest that bond (Bi-Cl)1 may have been broken under large tensile strains and there may be a competition between the intralayer and interlayer Bi-Cl bond while strain is applied. However, bond Bi-O and Cl-Cl nearly have no evident changes under strains, which comes from the strong covalent characteristics of Bi-O bonding and weak Cl-Cl interaction under strains. The parameters related to the vdW interactions ((Bi-Cl)2 and Cl-Cl)of bilayer BiOCl are bigger than that of bulk (monolayer) under strains that result from the quantum size effect (the vdW interactions). This is considered benefiting to its phase transformations which affects its unusual band structures.

Figure5c shows the interlamellar spacings Δ1, Δ2 and Δ3 of the layer only contains Bi-O-Bi atoms, Bi-Cl atoms and Cl-Cl atoms, respectively. We can see thatΔ3 (the vdW layer) and Δ1 (only contains Bi-O covalent bonding) decrease from compressive strain to tensile strain. The decrease of Δ1may related with the covalent bonding of Bi-O, decreasing angle (Bi-O-Bi)1 and increasing angle (Bi-O-Bi)2 (shown in Figure S3). Remarkably, Δ3 and Δ1 nearly declined into zero as the strain changes, indicating that the layer Bi-O-Bi (Δ1) turns to a flat and the vdW layer Cl-Cl (Δ3) is disappeared. Δ2 slightly decreases under small tensile strains but becomes larger while strain is changed into 15%, then even larger than the original vdW layer Δ3 at 30%. This indicates that a new vdW layer Δ2 has formed under large tensile strain and the original vdW layer Δ3 has meanwhile disappeared. This is consistent with the bond breaking of (Bi-Cl)1 under the large tensile strains we mentioned previously. With the similar mechanism of bond analysis which related to vdW

interactions for bilayer BiOCl ((Bi-Cl)2 and Cl-Cl), Δ3 is found to be larger than that of bulk and monolayer under strains. Overall, the changes of bond length, angle, and the interlamellar spacings are critical for the transformation of band structures, especially the bonds (Bi-Cl)1 and (Bi-Cl)2.As we discussed above, the competition between (Bi-Cl)1 and (Bi-Cl)2 plays an important role in the conversion of the band structure.

3.4. Band Decomposed Charge Density of Layered BiOCl with Different Strains

As discussed in section 3.2, the band transformations are mainly result from the energy changing of CBM-Λ, CBM-M, VBM-Γ, and VBM-Π under tensile strain and CBM-M, VBM-Ω, and VBM-M under compressive strain. To further clarify the mechanisms behind the band transformation under strains, the band decomposed charge density of these k points are calculated. According to our results, the differences of decomposed charge density among bulk, bilayer and monolayer are so tiny under strains, which can be ignored for simplicity. Hence, we only present the case of monolayer in Figure6.

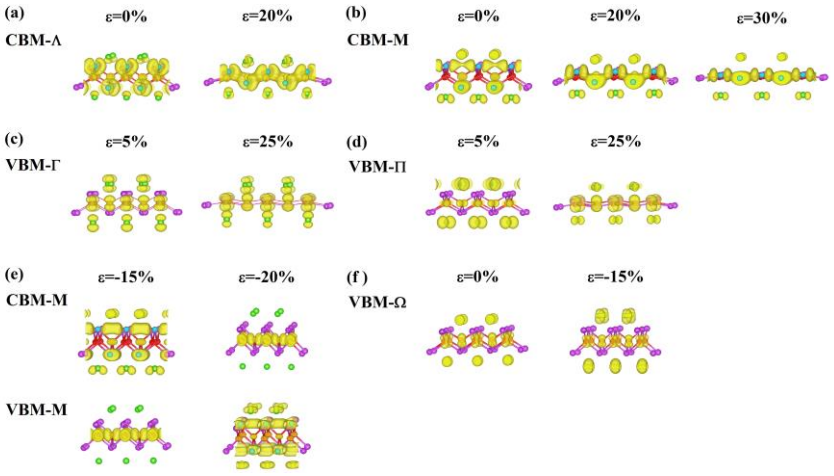

Figure 6. Band decomposed charge density of monolayer BiOCl at (a) CBM-Λ at strain 0%, 20% and (b) CBM-M at 0%, 20%, 30% (c) VBM-Γ at 5%, 25% and (d) VBM-Π at 5%, 25% under biaxial tensile strain. Band decomposed charge density of monolayer BiOCl at (e)CBM-M and VBM-M at -15%, -20% and (f) VBM-Ω at 0%, -15% under biaxial compressive strain.

In general, the stronger the hybridization of atoms is, the lower the energy is.[36] Figure 6 a and b illustrate that the hybridizations of CBM-Λ and CBM-M between Bi atoms become stronger as strain increases. Therefore, they are continuously declined as strain is applied on the band structures. In addition, it is obvious that the hybridizations of CBM-Λ are stronger than that of CBM-M at 20%, and as a result, CBM transfers to Λ at 20%. In parts c and d of Figure 6, the hybridization of VBM-Π between atoms increases as strain increases, and it grows stronger than VBM-Γ at 25%, which leads to the lower position of VBM-Π. These conversions result in the band structure transforms from indirect band to direct band under strains. Interestingly, the charge density of O at VBM-Π converts from p_{xy} to p_z which may relate to the flat-like Bi-O-Bi layer under large tensile strains.

As to compressive strain showed in Figure 6, parts e and f, the hybridization between Bi atoms for CBM-M becomes stronger as strain increases. This made the falling of state onM, lead to CBM finally transforms to M. The strong coexistence hybridization between Cl-p_x, Cl-p_y and Cl-p_z of VBM-Ω under strain -15% lead to the rapid dropping of VBM-Ω at -15%. Finally, the hybridization of VBM-Ω is stronger than VBM-M, leading to the VBM transforms from Ω to M. Furthermore, the charge density of Cl at VBM-Ω transform from p_{xy} to p_z, this results from the competition between bonds (Bi-Cl)1 and (Bi-Cl)2 which connected with Cl atoms. Another fantastic phenomenon is the charge density inversion between VBM-M and CBM-M at 20%. This means that it has an semiconductor-metal transition (SMT) at high compressive strains.

4. Conclusion

In summary, we performed first-principle-based theoretical investigations to gain insight into the influence of strains on the crystal, electronic and bonding properties of BiOCl. The band structure and formation energy calculations of BiOCl with different layers indicate that only a quantum size effect is observed and monolayer is still stable

with the layer number decreases from bulk to single-layer. The indirect-direct band transformations are found while the biaxial tensile and compressive strains are applied on BiOCl. This decisively depends on the energy up-shifting or down-shifting of the k-points at VBM or CBM under strains, which result from the various hybridizations between atoms. The phase transformation is found at high tensile strains only for bilayer because of its nonperiodic vdW interactions along the z axis. Particularly, our results predict an semiconductor-metal transition (SMT) at high compressive strainsfor all crystals. The calculations of bond length and interlayer spacing suggest that the competition between bond (Bi-Cl)1 and (Bi-Cl)2 should be the main reason which induce the band structure transformations. This paper may provide new insight for the design of BiOCl from the perspective of semiconductor devices.

Associated Content

Supporting Information

Formation energy of monolayer, bilayer and bulk BiOCl under strains, band structures of bulk BiOCl under biaxial compressive and tensile strains, and schematic illustrations of bond angle θX and the calculation results for bulk, bilayer and monolayer under tensile and compressive strains (PDF).

Author Information

Corresponding Author

*(W.H.)E-mail:whao@buaa.edu.cn.

*(Q. Z.) E-mail: qianfan@buaa.edu.cn.

Notes

The authors declare no competing financial interest.

Acknowledgments

This work was financially supported by the National Natural Science Foundation of China (NSFC) (Grant Nos. 51472016 and 51272015), Beijing Key Discipline

Foundation of Condensed Matter Physics. Q. Z. expresses thanks for the partial support by the Specialized Research Fund for the Doctoral Program of Higher Education of China (Grant No. 20131102120001), the National Natural Science Foundation of China (11404017), and the program for New Century Excellent Talents in University (Grant No. NCET-12-0033). Y.D., and S. D. thank the Australian Research Council (ARC) for partial support of this work through a Discovery Project (DP140102581).

References

(1) Butler, S. Z.; Hollen, S. M.; Cao, L.; et al. Progress, Challenges, and Opportunities in Two-dimensional Materials beyond Graphene. *ACS Nano***2013**, 7, 2898-2926.

(2) Bonaccorso, F.; Colombo, L.; Yu, G.; et al. Graphene, Related Two-dimensional Crystals, and Hybrid Systems for Energy Conversion and Storage. *Science*, **2015**, 347, 1246501.

(3) Zhou, J. J.; Feng, W.; Liu, C. C.; et al. Large-Gap Quantum Spin Hall Insulator in Single Layer Bismuth Monobromide Bi_4Br_4. *Nano Lett*. **2014**, 14, 4767-4771.

(4) Ma, Y.; Dai, Y.;Guo, M.; et al. Evidence of The Existence of Magnetism in Pristine VX_2Monolayers (X= S, Se) and Their Strain-induced Tunable Magnetic Properties. *ACS Nano* **2012**, 6, 1695-1701.

(5) Wang, Q. H.; Kalantar-Zadeh, K.; Kis, A.; et al. Electronics and Optoelectronics of Two-dimensional Transition Metal Dichalcogenides. *Nat. Nanotechnol.* **2012**, 7, 699-712.

(6) Wang, X.; Maeda, K.; Thomas, A.; et al. A Metal-free Polymeric Photocatalyst for Pydrogen Production from Water under Visible Light. *Nat. Mater.* **2009**, 8, 76-80.

(7) Liu, Z.; Lou, Z.; Li, Z.; et al. GeH: ANovel Material as A Visible-light Driven Photocatalyst for Hydrogen Evolution. *Chem. Commun.* **2014**, 50, 11046-11048.

(8) Li, L.; Salvador, P. A.; Rohrer, G. S.;Photocatalysts with Internal Electric Fields. *Nanoscale* **2014**, 6, 24-42.

(9) An, H.Z.; Du, Y.; Wang, T. M.; et al. Photocatalytic Properties of BiOX (X=Cl, Br,

and I). *Rare Met.*, **2008**, 27, 243-250.

(10)Zhang, K. L.; Liu, C. M.; Huang, F. Q.; et al. Study of the Electronic Structure and Photocatalytic Activity of the BiOCl Photocatalyst. *Appl. Catal. B.* **2006**, 68, 125-129.

(11) Zhang, X.; Ai, Z,; Jia, F.; et al. Generalized One-pot Synthesis, Characterization, and Photocatalytic Activity of Hierarchical BiOX (X=Cl, Br, I) Nanoplate Microspheres. *J. Phys. Chem. C* **2008**, 112, 747-753.

(12) Guan, M.; Xiao, C.; Zhang, J.; et al. Vacancy Associates Promoting Solar-driven Photocatalytic Activity of Ultrathin Bismuth Oxychloride Nanosheets. *J. Am. Chem. Soc.* **2013**, 135, 10411-10417.

(13) Zhang, X.; Li, B.; Wang, J.; et al. The Stabilities and Electronic Structures of Single-layer Bismuth Oxyhalides for Photocatalytic Water Splitting. *Phys. Chem. Chem.Phys.* **2014**, 16, 25854-25861.

(14) Jiang, J.; Zhao, K.; Xiao, X.; et al. Synthesis and Facet-dependent Photoreactivity of BiOCl Single-crystalline Nanosheets. *J. Am. Chem. Soc.* **2012**, 134, 4473-4476

(15) Yang, W.; Wen, Y.; Chen, R.; et al. Study of Structural, Electronic and Optical Properties of Tungsten Doped Bismuth Oxychloride by DFT Calculations. *Phys. Chem. Chem. Phys.* **2014**, 16, 21349-21355.

(16) Zhou, D.; Pu, C.; He, C.; et al. Pressure-induced Phase Transition of BiOF: Novel Two-dimensional Layered Structures. *Phys. Chem. Chem. Phys.* **2015**, 17, 4434-4440.

(17) Ju, W.; Li, T.; Wang, H.; et al. Strain-induced Semiconductor to Metal Transition in Few-layer Black Phosphorus from First Principles. *Chem. Phys. Lett.*, **2015**, 622, 109-114.

(18) Zhang, S.; Yan, Z.; Li, Y.; et al. Atomically Thin Arsenene and Antimonene: Semimetal-Semiconductor and Indirect-Direct Band-Gap Transitions. *Angew. Chem.*, **2015**, 127, 3155-3158.

(19) Peng, X. H.; Alizadeh, A.; Bhate, N.; et al. First-principles Investigation of Strain Effects on the Energy Gaps in Silicon Nanoclusters. *J. Phys.: Condens. Matter*

2007, 19, 266212.

(20) Rodin, A. S.; Carvalho, A.; Neto, A. H. C. Strain-induced Gap Modification in Black Phosphorus. *Phys. Rev. Lett.* **2014**, 112, 176801.

(21) Çakır, D.; Sahin, H.; Peeters, F. M.; Tuning of the Electronic and Optical Properties of Single-layer Black Phosphorus by Strain. *Phys. Rev. B: Condens. Mater. Phys.* **2014**, 90, 205421.

(22) Scalise, E.; Houssa, M.; Pourtois, G.; et al. Strain-induced Semiconductor to Metal Transition in the two-dimensional Honeycomb Dtructure of MoS_2. *Nano Res.* **2012**, 5, 43-48.

(23) Feng H F, Xu Z F, Wang L, et al. Modulation of Photocatalytic Properties by Strain in 2D BiOBrNanosheets. *ACS Appl. Mater. Interfaces*, **2015**, 7 (50), 27592–27596

(24) Keramidas, K. G.; Voutsas, G. P.; Rentzeperis, P. I. The Crystal Structure of BiOCl.*Z.Kristallogr.-Cryst.Mater.*, **1993**, 205, 35-40.

(25) Zhang, K. L.; Liu, C. M. Huang, F. Q.; et al. Study of the Electronic Structure and Photocatalytic Activity of the BiOCl Photocatalyst. *Appl. Catal. B* **2006**, 68, 125-129.

(26) Yan, J. A.; Xian, L.; Chou, M. Y.; Structural and Electronic Properties of Oxidized Graphene. *Phys. Rev. Lett.* **2009**, 103, 086802.

(27) Reich, S.; Li, L.; Robertson, J. Structure and Formation Energy of Carbon Nanotube Caps. *Phys. Rev. B: Condens. Matter. Phys.* **2005**, 72, 165423.

(28) Kuc, A.; Zibouche, N.; Heine, T.; Influence of Quantum Confinement on the Electronic Structure of the Transition Metal Sulfide TS_2. *Phys. Rev. B: Condens. Matter. Phys.* **2011**, 83, 245213.

(29) Malone B. D.; Louie S. G.; Cohen M. L.;Electronic and Optical Properties of Body-centered-tetragonal Si and Ge. *Phys. Rev. B: Condens. Matter. Phys.* **2010**, 81, 115201.

(30) Duan D.; Liu Y.; Tian F.; et al. Pressure-induced Metallization of Dense$(H_2S)_2H_2$ with high-Tc Superconductivity. *Sct. Rep.,* **2014**, 4, 6968.

(31) Drozdov A. P.; Eremets M. I.;Troyan I. A.; et al. Conventional

Superconductivity at 203 Kelvin at HighPressures in the Sulfur Hydride System. *Nature*, **2015**, 525, 73–76.

(32) Li Y. W.; Hao J.; Liu H. Y.; et al. The Metallization and Superconductivity of Dense Hydrogen Sulfide. *J. Chem. Phys.* **2014**, 140, 174712.

(33) Deng H. Y.; Hao W. C.; Xu H. Z.; Wang. C. Effect of Intrinsic Oxygen Vacancy on the Electronic Structure of γ-Bi2O3: First-Principles Calculations. *J. Phys. Chem. C* **2012**, 116, 1251–1255.

(34) Peng, X.; Wei, Q.; Copple, A.; Strain-engineered Direct-indirect Band Gap Transition and Its Mechanism in Two-dimensional Phosphorene. *Phys. Rev. B: Condens. Matter. Phys.* **2014**, 90, 085402.

(35) Fan, X.; Chang,C. H.; Zheng, W.; et al. The Electronic Properties of Single-layer and Multi-layer MoS2 under High Pressure. *J. Phys. Chem. C* **2015**, 119, 10189–10196.

(36) Johari, P.; Shenoy, V. B. Tuning the Electronic Properties of Semiconducting Transition Metal Dichalcogenides by Applying Mechanical Strains. *ACS Nano* **2012**, 6, 5449-5456.

Figure Captions

Figure 1.Crystal structure of BiOCl. (a) side view, (b) top view.

Figure 2. (a) Formation energy and band gap, (b) band structure of BiOCl with bulk, 6-layer, 4-layer, 3-layer, bilayer and monolayer.

Figure 3. The crystal structures of bilayer under tensile strain at (a) 0%, (b) 25%, (c) 30%.

Figure 4.Band structure of (a) monolayer and (b) bilayer BiOCl under biaxial compressive, without and tensile strains.

Figure 5.(a) The schematic illustrations of bond length and interlamellar spacings, (b) bond length dX, (c) interlamellar spacings ΔX of bulk, bilayer and monolayer under tensile and compressive strains. Purple, red, green atoms respectively refer to Bi, O and Cl atoms.

Figure6. Band decomposed charge density of monolayer BiOCl at (a)CBM-Λ at strain 0%, 20% and (b) CBM-M at 0%, 20%, 30% (c) VBM-Γ at 5%, 25% (d)VBM-Π at 5%, 25% under biaxial tensile strain. Band decomposed charge density of monolayer BiOCl at (e)CBM-M and VBM-M at -15%, -20% and (f) VBM-Ω at 0%, -15%under biaxial compressive strain.

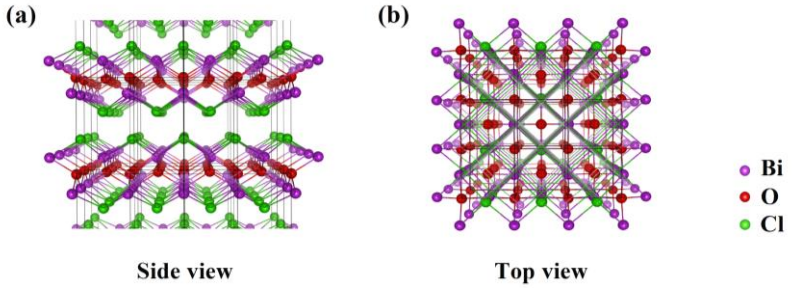

Figure 1.

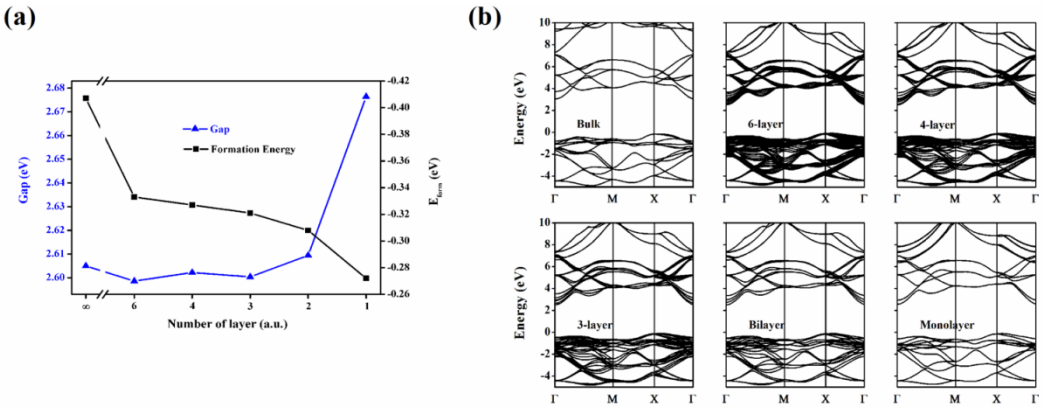
(a)
Gap
Formation Energy
Gap (eV)
E_{form} (eV)
Number of layer (a.u.)
(b)
Bulk
6-layer
4-layer
3-layer
Bilayer
Monolayer
Energy (eV)
Γ M X Γ

Figure 2.

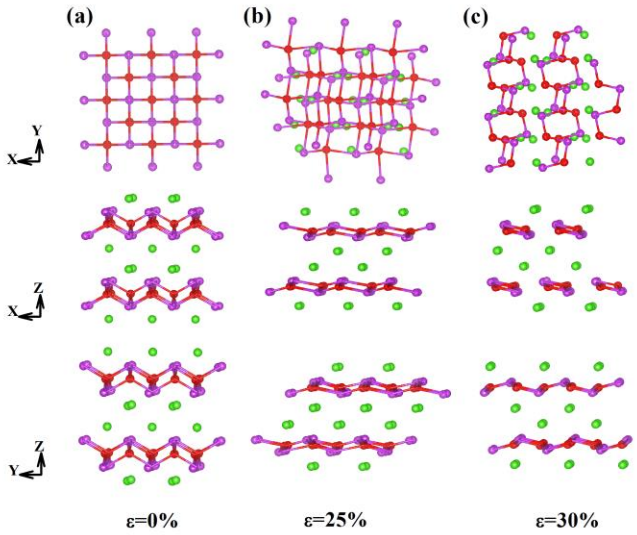

Figure 3.

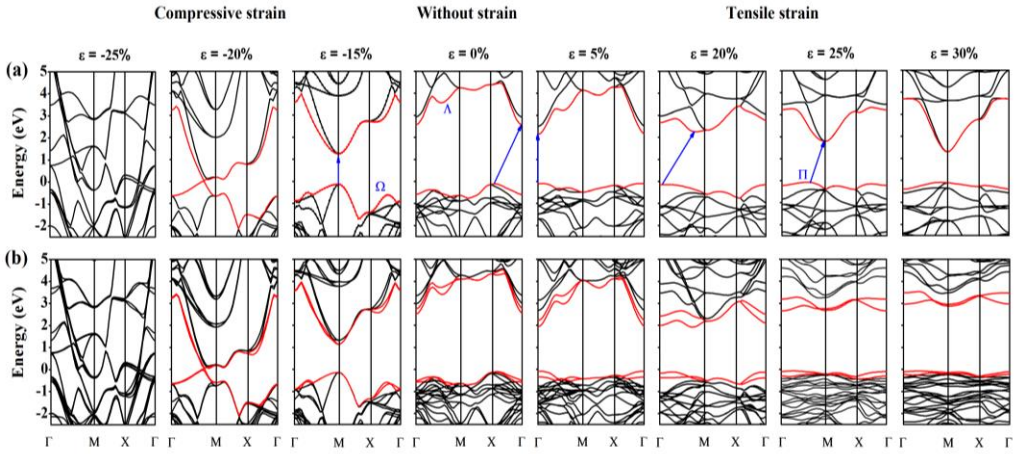
Compressive strain
Without strain
Tensile strain
ε = -25%
ε = -20%
ε = -15%
ε = 0%
ε = 5%
ε = 20%
ε = 25%
ε = 30%
(a)
(b)
Energy (eV)
Λ
Ω
Π
Γ M X Γ

Figure 4.

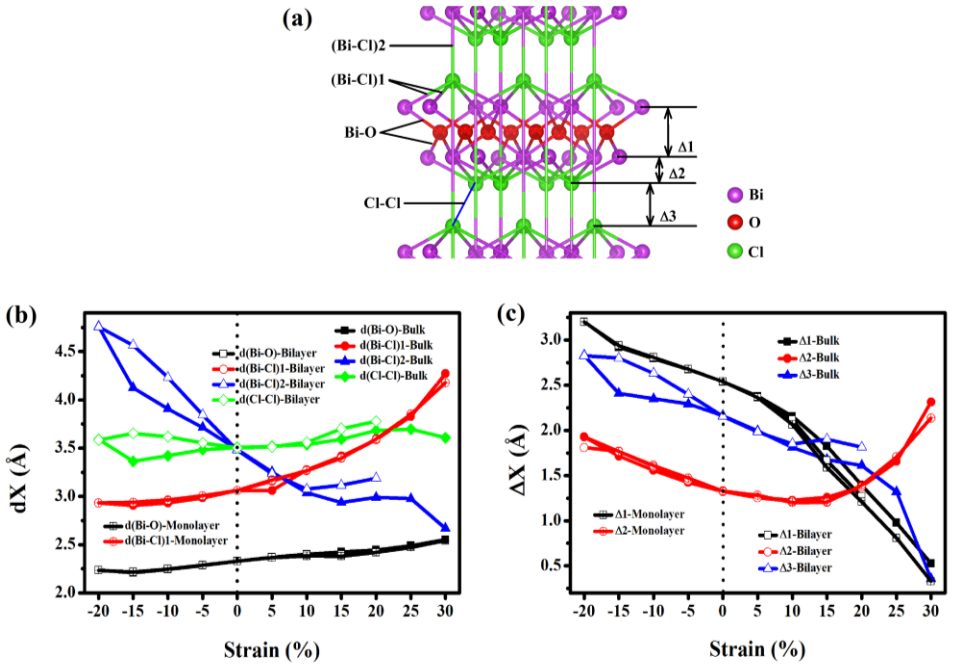
(a)
(Bi-Cl)2
(Bi-Cl)1
Bi-O
Cl-Cl
Δ1
Δ2
Δ3
Bi
O
Cl
(b)
dX (Å)
Strain (%)
d(Bi-O)-Bulk
d(Bi-Cl)1-Bulk
d(Bi-Cl)2-Bulk
d(Cl-Cl)-Bulk
d(Bi-O)-Bilayer
d(Bi-Cl)1-Bilayer
d(Bi-Cl)2-Bilayer
d(Cl-Cl)-Bilayer
d(Bi-O)-Monolayer
d(Bi-Cl)1-Monolayer
(c)
ΔX (Å)
Strain (%)
Δ1-Bulk
Δ2-Bulk
Δ3-Bulk
Δ1-Monolayer
Δ2-Monolayer
Δ1-Bilayer
Δ2-Bilayer
Δ3-Bilayer

Figure 5.

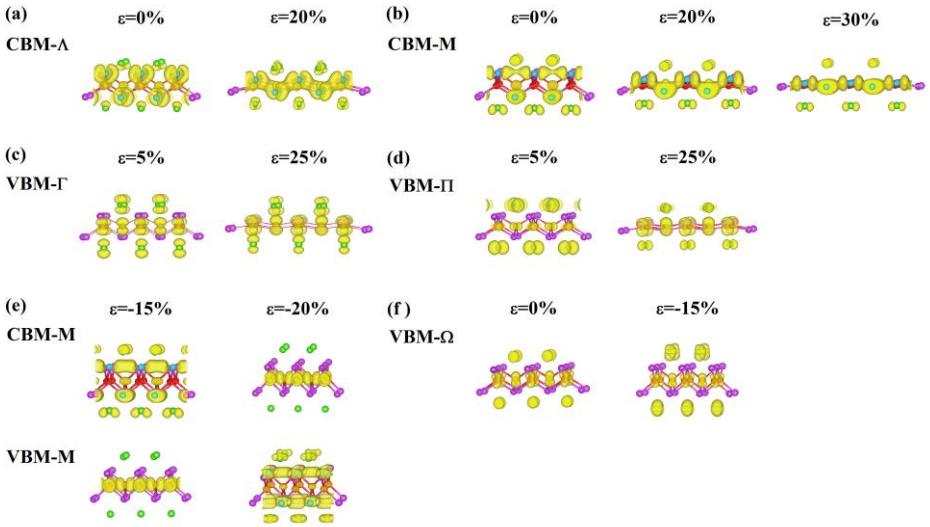
(a)
ε=0%
ε=20%
CBM-Λ
(b)
ε=0%
ε=20%
ε=30%
CBM-M
(c)
ε=5%
ε=25%
VBM-Γ
(d)
ε=5%
ε=25%
VBM-Π
(e)
ε=-15%
ε=-20%
CBM-M
VBM-M
(f)
ε=0%
ε=-15%
VBM-Ω

Figure 6.

Table of Contents Image